

Research Article

Blockchain-Based Privacy Access Control Mechanism and Collaborative Analysis for Medical Images

Puja Sahay Prasad ¹, G N Beena Bethel ², Ninni Singh ³, Vinit Kumar Gunjan ³, Samar Basir ³, and Shahajan Miah ⁴

¹Department of Computer Science and Engineering, Geethanjali College of Engineering and Technology, Hyderabad, India

²Department of Computer Science and Engineering, Gokaraju Rangaraju Institute of Engineering and Technology, Hyderabad, India

³Department of Computer Science and Engineering, CMR Institute of Technology, Hyderabad, India

⁴Department of EEE, Bangladesh University of Business and Technology (BUBT), Dhaka, Bangladesh

Correspondence should be addressed to Shahajan Miah; miahbubt@bubt.edu.bd

Received 9 February 2022; Revised 12 April 2022; Accepted 26 April 2022; Published 29 June 2022

Academic Editor: Mukesh Soni

Copyright © 2022 Puja Sahay Prasad et al. This is an open access article distributed under the Creative Commons Attribution License, which permits unrestricted use, distribution, and reproduction in any medium, provided the original work is properly cited.

Medical image analysis technology based on deep learning has played an important role in computer-aided disease diagnosis and treatment. Classification accuracy has always been the primary goal pursued by researchers. However, the image transmission process also faces the problems of limited wireless ad-hoc network (WAN) bandwidth and increased security risks. Moreover, when user data are exposed to unauthorized users, platforms can easily leak personal privacy. Aiming at the abovementioned problems, a system model and an access control scheme for the collaborative analysis of the diagnosis of diabetic retinopathy (DR) are constructed in this paper. The system model includes two stages of data cleaning and lesion classification. In the data cleaning phase, the private cloud writes the model obtained after training into the blockchain, and other private clouds use the best-performing model on the chain to identify the image quality when cleaning data and pass the high-quality image to the lesion classification model for use. In the lesion classification stage, each private cloud trains the classification model separately; uploads its own model parameters to the public cloud for aggregation to obtain a global model; and then sends the global model to each private cloud to achieve collaborative learning, reduce the amount of data transmission, and protect personal privacy. Access control schemes include improved role-based access control (RAC) used within the private cloud and blockchain-based access control used during the interaction between the private cloud and the public cloud program (BAC). RAC grants both functional rights and data access rights to roles and takes into account object attributes for fine-grained level control. Based on certificateless public-key encryption technology and blockchain technology, BAC can realize the identity authentication and authority identification of the private cloud while requesting the transmission of model parameters from the private cloud to the public cloud and protect the security of the identity, authority, and model parameters of the private cloud to achieve the effect of lightweight access control. In the experimental part, two retinal datasets are used for DR classification analysis. The results show that data cleaning can effectively remove low-quality images and improve the accuracy of early lesion classification for doctors, with an accuracy rate of 90.2%.

1. Introduction

With the development of digital medicine and machine learning, more and more e-health systems are favored by academia and industries. Due to the digital nature, much

medical data need to be stored electronically and shared through cloud platforms for higher quality and broader applications. The medical image analysis process is usually based on the identification of doctors or experts. Still, it is easy to cause visual fatigue, which leads to a decrease in

identification accuracy. Deep learning algorithms, especially convolution neural networks, can automatically learn more specific features to improve classification accuracy. Therefore, it has quickly become a research hotspot for analyzing medical images [1]. However, the amount of image data will affect the model training accuracy and it is not easy to gather all the photos of all hospitals together in reality. Scholars have proposed deep collaborative learning to improve the classification accuracy and applied it in medical image analysis [2]. However, in these medical image data processing systems with independent private clouds, user data are easily exposed to illegal users [3]. Access control set of access rules can ensure that authorized users can access resources and unauthorized users cannot access them to solve the problems of data security and privacy leakage [4].

In the past, people have used deep learning or collaborative deep learning algorithms to analyze medical images. A feature transfer network and local background suppression-based method for microaneurysm detection, for example, is proposed in literature [5]. A deconvolutional neural network, on the other hand, is proposed in literature [6]. Using morphological opening and closing operations, reference [7] can get rid of isolated noise points. To make training and test sets, for example, a method of comparing the size of each picture is used. As an example, the literature [8] came up with a collaborative deep learning model to help people figure out which lung nodules are malignant and which are not, even though they have limited chest CT data. This model is based on multiview knowledge [9] based on two collaborative convolutional neural network models; this section proposes an automatic segmentation algorithm for shoulder joint images that can accurately segment the glenoid and humeral head in shoulder collective images [10]. This section proposes a segmentation learning method for deep learning of healthcare collaboration. However, the existing deep learning and collaborative deep learning algorithms only think about how to make models. So, it does not take into account how data cleaning and classification work together, which will lead to low data quality. There are also issues with personal privacy and data security.

2. Related Work

Scholars have come up with a variety of ways to keep medical data safe and private. For example, in literature [11], there is a way to control access to medical images by using a two-layer system. S. M. Islam and others came up with a risk-based access control model that changes as people get more or less access. Role-based access control (RBAC), attribute-based access control (ABAC), and blockchain-based access control are some of the most common access control models (blockchain-based access control, BBAC). RBAC uses the user's role to set a security policy and the procedure is usually linked to the user's job. This is common in a hospital information system (HIS) that is used in the real world. Literature [11] came up with a way to control access to a cloud infrastructure-as-a-service based on roles. N. Weng and his team came up with a way to get reasonable fine-grained access control. They came up with the attribute-

based controlled collaborative access control (ABCCCC) model. The data owner chooses a group of people to collaborate with. In [12], attribute-based fine-grained access control encryption is designed to mark ciphertexts with attribute sets so that only certain people can read them. Because of the blockchain's decentralization and immutability, it is a good idea to use it to solve problems with electronic medical records' interoperability and security [13]. Blockchain-based access control methods have been used in some medical information systems before. In [14], a design that is both scalable and robust is shown. It uses blockchain technology for access control. It uses a discrete wavelet transform method to make it more secure. Blockchain was used by O. Oktay et al. to keep patient health records safe and private, which solved the problem of losing control when encrypting data [15]. Some works do not pay attention to how fine-grained access is at the attribute level. For BBAC, many pieces do not pay attention to the fact that they are lightweight. So, the performance and scalability of their scheme are limited by complicated consensus mechanisms that take a lot of time.

Two access control schemes are proposed in this paper to keep people from getting their hands on medical data without permission. One is an improved role-based access control (RAC) scheme and the other is a blockchain-based access control (BAC) scheme. RAC is based on how important a role is, with attribute-level constraints that keep people who are not supposed to be able to access the HIS from doing so. BAC uses blockchain technology to keep third-party trusted third-party authorities out of the distributed network architecture, which does not need them. Access control policies use a lightweight certificateless public-key encryption algorithm to protect medical data's security, as well as to cut down on the amount of data that needs to be sent. So that other systems used are more secure and have enough bandwidth, because most of the HIS's functions are done on the local network. For example, when using the system functions on a LAN, the role-based access control scheme is used. The lightweight access control scheme based on blockchain, however, is used when using system functions for WAN.

3. Deep Learning for Classification

The quality of clinical medical images is uneven and low-quality color fundus images mainly have problems such as low contrast, overexposure, and noise in the picture. These low-quality images significantly increase the difficulty of diagnosis for ophthalmologists and even cannot distinguish the types of lesions in the early stage of DR, such as bleeding spots and hard exudates. At the same time, when using computer technology to detect DR lesions automatically, low-quality color fundus images will significantly interfere with the training process of the detection model, so that a model for accurate detection of lesions cannot be trained. Therefore, culling these low-quality images in the data cleaning stage can significantly improve model detection. In this paper, the CNN model is used to detect low-quality

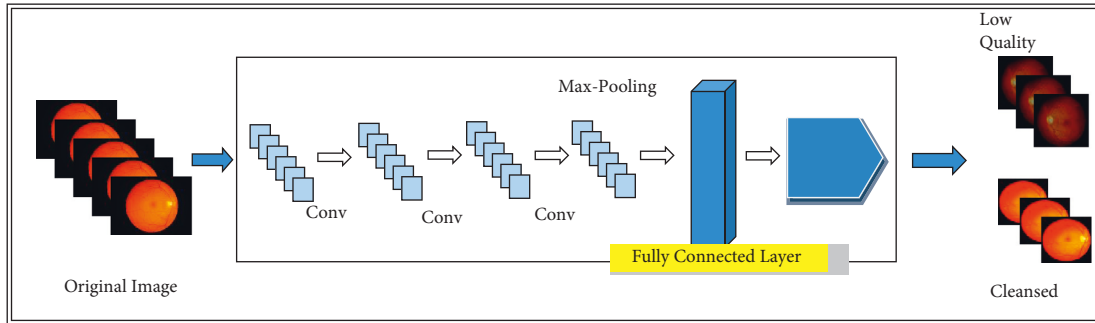


FIGURE 1: Data cleaning model.

TABLE 1: Data cleaning model parameters.

Floor	Type	Feature map size	Filter size	Step size	Number of parameters
0	Input	$88 \times 88 \times 3$	—	—	—
1	Convolution layer	$88 \times 88 \times 24$	$5 \times 5 \times 24$	1	624
2	Convolution layer	$80 \times 80 \times 16$	$3 \times 3 \times 16$	1	160
3	Convolution layer	$78 \times 78 \times 8$	$3 \times 3 \times 8$	1	80
4	Max-pooling	$39 \times 39 \times 8$	2×2	2	—
5	Fully connected layer	64	—	—	778688
6	Fully connected layer	2	—	—	126

TABLE 2: Comparison of role-based access control.

Model	RBAC (proposed)	ABCCC [17]	E-RBAC [18]	SAT-RBAC [19]	ABAC-IaaS [20]
Support attribute	Support	Support	Not support	Not support	Support
Flexibility	High	Low	High	Low	Generally
Dynamism	High	Low	Low	Low	High
Extensibility	High	Low	Low	Low	High
Multilevel security control	Support	Support	Not support	Not support	Not support
Model safety	High	High	Low	Generally	Low

photos. The model structure is shown in Figure 1, and the model parameters are shown in Table 1. In this paper, the model in [16] is used to detect bleeding points and hard exudates in fundus images, and the detection effect is better than most of the existing methods.

4. Experiments and Result Analysis

4.1. Comparison of RBAC Schemes. Table 2 lists some role-based access control models and compares them with the RAC model in this paper in terms of attribute-based, flexibility, and dynamism. The RAC model proposed in this paper can be flexibly configured when controlling data domain access. Different levels of roles can realize data access in different scopes. Functional operations can be increased or decreased according to business needs. It has the characteristics of flexibility, dynamism, and scalability. It has been applied in practical projects and proved available and convenient. In addition, RAC enables fine-grained access control based on attributes. As shown from Table 2, RAC is superior to ABCCC, E-RBAC/SAT-RBAC, and ABAC-IaaS in terms of whether to support attribute-level power, flexibility, dynamism, scalability, multilevel security control, and model security.

4.2. Comparison of Running Time in BAC. The runtime comparison tests were done on a computer with the Windows 10 operating system that had a 2.9 GHz Intel(R) Core(TM) i7-7500U, 8 Gb RAM, 128 Gb SSD, and 1 Tb HDD. IDEA 2018.3.1 Ultimate Edition was used to write the code. Encryption and decryption, as well as signing and verifying, are based on ECIES and ECDSA. In Secp160r1, we use the parameters in Secp160r1 (SEC2) as a guide for the security strength of ECC with 160 bit keys. The algorithm for symmetric keys in Encrypt is 128 bit AES. If you want to figure out how much time it takes to do arithmetic operations like hashing and symmetric cryptography, you usually look at the number of scalar multiplications and the running time of each one (a scalar multiplication running time the average is about 0.81 ms).

In the BAC scheme, PE is encrypted/decrypted, signed, and authenticated with BL-CL-PKC. Compared to the literature, it encrypts L-CL-PKS and PKE with the literature [21–23] and PKS with the literature [16, 24–26], [27–29]. Figure 2(a) shows how long it takes the algorithm to do encryption and decryption on PE. The figure shows that the algorithm L-CL-PKE is better than the comparison algorithm when it comes to how long it takes to encrypt and decrypt a piece of data. As you can see in Figure 2(b), the

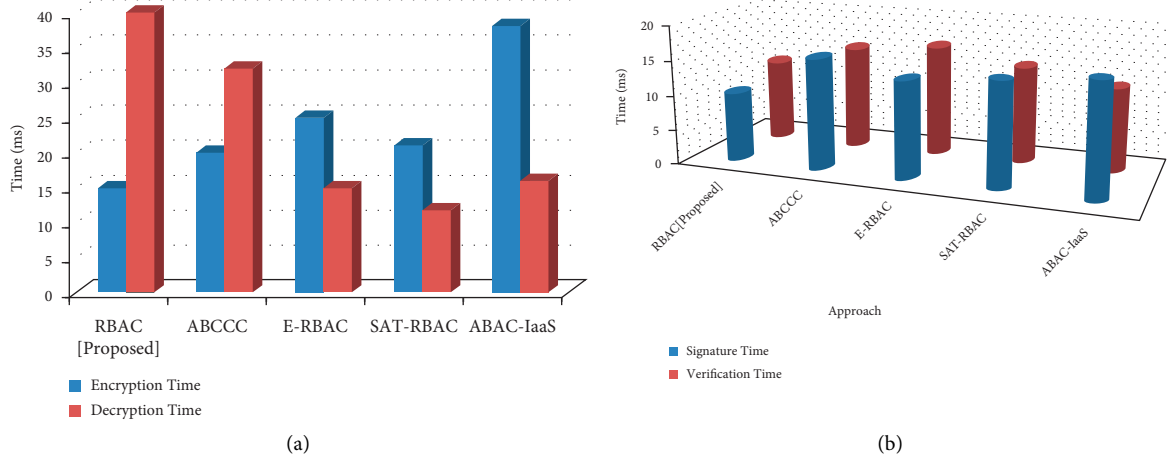


FIGURE 2: Time consumption comparison. (a) Encryption and decryption. (b) Signature and authentication.

algorithm's running time for PE signature and authentication operations is shown. L-CL-PKS is a better algorithm than the comparison algorithm when it comes to the time it takes to sign and authenticate a PE file, as shown in the figure. Due to the bilinear pairings used in CL-PKE, the running time is longer. Because the cost is more than scalar multiplication, the other algorithms have more scalar multiplication than this one [30]. On the other hand, the design of L-CL-PKE in this paper does not use identity-based encryption. Instead, it tries to make ECC work with ID instead. Still, it has the same features of identity-based public-key encryption. So, the proposed BAC scheme is very light. Table 3 shows the comparison between encryption and decryption time. Also, the comparison between signature and verification time is shown in Table 4.

4.3. Lesion Classification Results. DR early lesion detection is done on the fundus images in the DIARETDB1 (DB1) dataset in this paper. In this paper, data cleaning experiments are done on the DIARETDB0 (DB0) dataset. 130 color fundus images are in the DB0 dataset and 89 color fundus images are in the DB1 dataset. The size of the fundus images in both datasets is $1500 * 1152$. Images in DB0 are broken down into low-quality and high-quality ones. The DB0 dataset is used to train the model that cleans data. To see how well the model works, this paper uses the DB1 dataset to test the model that was trained. The results of the experiments show that the model chosen in this paper can filter out low-quality fundus images and its accuracy can be increased to 74.4%. It also has ground truth maps of bleeding spots and hard exudates, which are used to check the model's lesion classification. At the same time, this paper uses the 10-fold cross-validation method to both train and test the model and it does both. The sensitivity and accuracy of the detection results are two of the measurement standards. It is the percentage of correct positive samples to all correct positive samples. It is used to see how well the model can predict which positive samples will be correct. It is the ratio of the number of positive and negative examples correctly classified to the sum of all positive and negative examples. It is

TABLE 3: Comparative encryption and decryption time.

Approach	Time (MS)	
	Encryption time	Decryption time
RBAC (proposed)	15	40
ABCCC	20	32
E-RBAC	25	15
SAT-RBAC	21	12
ABAC-IaaS	38	16

TABLE 4: Signature and verification time.

Approach	Time (milliseconds)	
	Signature time	Verification time
RBAC (proposed)	10	12
ABCCC	16	15
E-RBAC	14	16
SAT-RBAC	15	14
ABAC-IaaS	16	12

used to figure out how well the whole model classification did. The following are the ways to do:

$$\text{Sensitivity} = \frac{TP}{TP + FN}, \quad (1)$$

$$\text{Accuracy} = \frac{TP + TN}{TP + FN + TN + FP},$$

where TP is the correctly predicted positive sample, TN is the correctly predicted negative sample, FP is the incorrectly predicted positive sample, and FN is the incorrectly predicted negative sample. In this experiment, the detection accuracy of the positive and negative models reached 90.2%. Sensitivity is the detection effect of one of the color fundus images. Figure 3 shows classification results of bleeding spots and hard exudates on the DB1 dataset.

In addition to sensitivity and accuracy, this paper also uses the ROC curve to measure the detection effect of different lesions, which depicts the relationship between sensitivity and the average number of false detections per

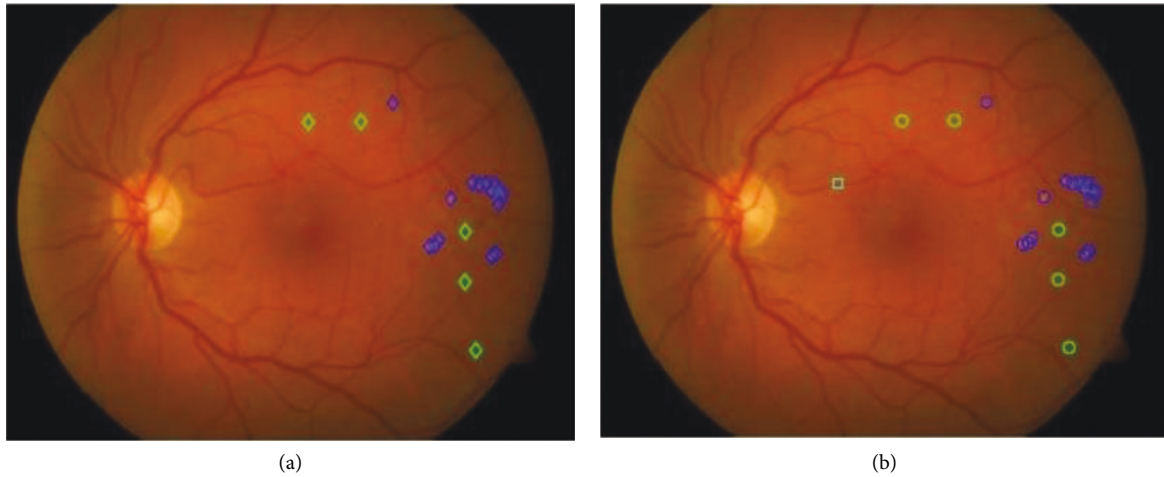


FIGURE 3: Classification results of bleeding spots and hard exudates on the DB1 dataset. (a) Raw retinal image. (b) Classification results.

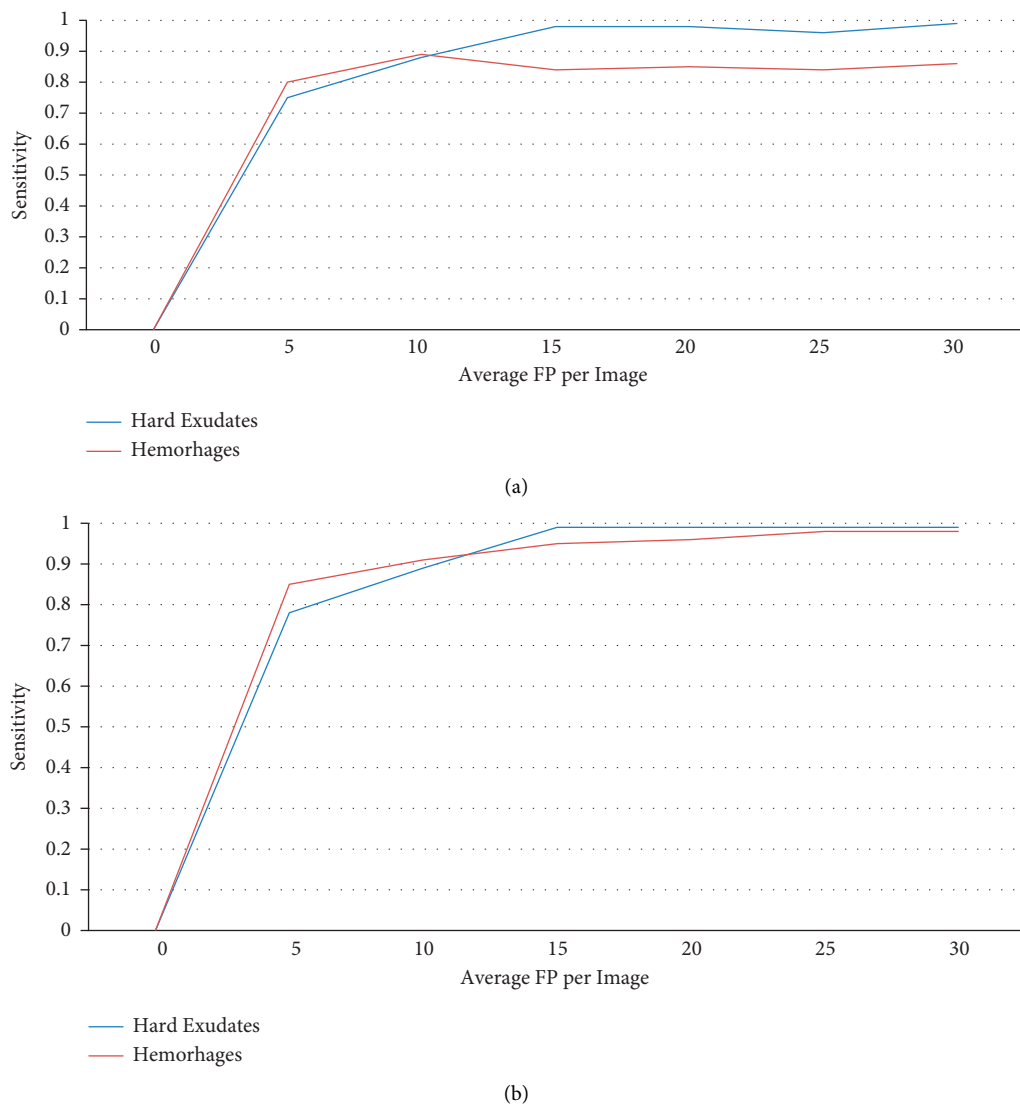


FIGURE 4: ROC curves for DR lesion classification. (a) ROC curve without data cleaning. (b) ROC curve using data cleaning.

TABLE 5: Sensitivity without data cleaning.

FP/Image	Hard exudates	Hemorrhages
0	0	0
5	0.75	0.8
10	0.88	0.89
15	0.98	0.84
20	0.98	0.85
25	0.96	0.84
30	0.99	0.86

TABLE 6: Sensitivity with data cleaning.

FP/Image	Hard exudates	Hemorrhages
0	0	0
5	0.78	0.85
10	0.89	0.91
15	0.99	0.95
20	0.99	0.96
25	0.99	0.98
30	0.99	0.98

TABLE 7: Detection sensitivity of DR lesions (1000 iteration).

Approach	Hemorrhages	Hard exudates
No data cleaning	0.8564	0.9623
RBAC (proposed)	0.9125	0.9845
ABCCC	0.6265	0.8766
E-RBAC	0.5264	0.8304
SAT-RBAC	0.5856	0.8205
ABAC-IaaS	0.840	0.8045

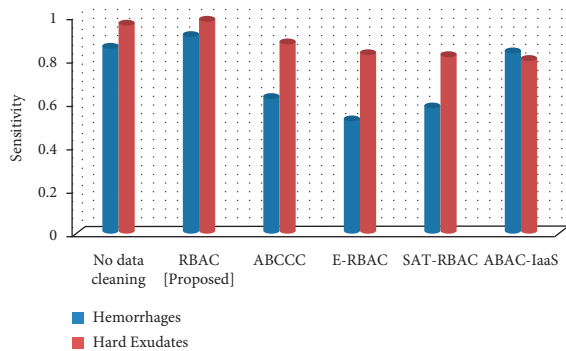


FIGURE 5: Detection sensitivity of DR lesions (1000 iteration).

image. Figures 4(a) and 4(b) depict the ROC curves before and after data cleaning. It can be seen from the angles that the detection sensitivity of different lesions is improved after cleaning. Tables 5 and 6 show the sensitivity without and with data cleaning, respectively.

Sensitivity for each lesion is listed in Table 7, with increased sensitivity for bleeding spots and hard exudates after data cleaning. This has been shown graphically in Figure 5. To more objectively verify the detection performance of this model, this paper also compares the detection of fundus images by different existing methods, as shown in Table 5. It can be seen from the table that the bleeding points are hard

exudates after data cleaning. The sensitivity of this model has been improved and the detection performance of this model is better than other existing methods, which shows the effectiveness of this method for fundus target detection.

5. Conclusion

This paper designs a medical image collaborative analysis system model based on deep learning, which can protect the security of medical data and model parameters, reduce the amount of data transmission, save bandwidth, and achieve more accurate lesion classification. The first stage in the system model is data cleaning, that is, the doctor collects images, uploads them to the private cloud for data cleaning, and transfers the cleaned high-quality images to the classification model; the second stage is classification, that is, the private cloud uses high-quality images to perform model training, upload the model parameters to the public cloud for aggregation, and then the public cloud will transfer the newly obtained global model to the private cloud. This paper designs two access control schemes in these two stages, RAC and BAC. RAC can implement fine-grained, flexible, and dynamic access control based on roles and attributes. BAC is a blockchain-based solution that eliminates trusted third parties to prevent single-point-of-failure authentication or man-in-the-middle attacks. Based on certificates, the public-key encryption technology enables light data transmission over WAN. In addition, when the private cloud requests to upload model parameters from the public cloud, it does not need to perform identity authentication and authority identification separately but encapsulates the identity and authority information together with the model parameters to reduce the separate identity identification operation. Both schemes prevent unauthorized users from accessing medical data. Data cleaning can remove low-quality images to diagnose early DR lesions and effectively improve accuracy. The experimental results and security analysis prove that the scheme can effectively protect the system's security to classify medical data, and the classification accuracy can reach 90.2%.

Data Availability

The data will be made available on request from corresponding author.

Conflicts of Interest

The authors declare that they have no conflicts of interest.

References

- [1] X. Guo, P. Zhang, C. Wang, B. Sun, and S. Sun, "A novel deep learning model for palmprint/palmvein recognition," *IEEE Access*, vol. 9, Article ID 122847, 2021.
- [2] Q. Yan, J. Huang, C. Xiong, Z. Yang, and Z. Yang, "Data-driven human-robot coordination based walking state monitoring with cane-type robot," *IEEE Access*, vol. 6, pp. 8896–8908, 2018.

- [3] B. T. Baker, R. F. Silva, V. D. Calhoun, A. D. Sarwate, and S. M. Plis, "Large scale collaboration with autonomy: decentralized data ICA," in *Proceedings of the IEEE 25th International Workshop on Machine Learning for Signal Processing (MLSP)*, pp. 1–6, Boston, MA, USA, September 2015.
- [4] Ieee, "IEE colloquium on 'medical imaging: image processing and analysis' (digest No.051)," in *Proceedings of the IEE Colloquium on Medical Imaging: Image Processing and Analysis*, London, UK, March 1992.
- [5] F. Ritter, "Medical image analysis," *IEEE Pulse*, vol. 2, no. 6, pp. 60–70, 2011.
- [6] S. K. Sen, M. Foskey, J. S. Marron, and M. A. Styner, "Support vector machine for data on manifolds: an application to image analysis," in *Proceedings of the 5th IEEE International Symposium on Biomedical Imaging*, pp. 1195–1198, Paris, France, May, 2008.
- [7] W. J. Niessen, B. M. T. H. Romeny, and M. A. Viergever, "Geodesic deformable models for medical image analysis," *IEEE Transactions on Medical Imaging*, vol. 17, no. 4, pp. 634–641, 1998.
- [8] W. Yuan, M. Hamit, A. Kutluk, and C. Yan, "Feature extraction and analysis on Xinjiang uygur medicine image by using color histogram," in *Proceedings of the IEEE International Conference on Medical Imaging Physics and Engineering*, pp. 259–264, Shenyang, China, October, 2013.
- [9] D. Tellez, G. Litjens, J. van der Laak, and F. Ciompi, "Neural image compression for gigapixel histopathology image analysis," *IEEE Transactions on Pattern Analysis and Machine Intelligence*, vol. 43, no. 2, pp. 567–578, 2021.
- [10] R. A. Brown, H. Zhu, and J. R. Mitchell, "Distributed vector Processing of a new local MultiScale Fourier transform for medical imaging applications," *IEEE Transactions on Medical Imaging*, vol. 24, no. 5, pp. 689–691, 2005.
- [11] S. M. Islam and H. S. Mondal, "Image enhancement based medical image analysis," in *Proceedings of the 10th International Conference on Computing, Communication and Networking Technologies (ICCCNT)*, pp. 1–5, Kanpur, India, July, 2019.
- [12] O. Oktay, W. Bai, R. Guerrero, and M. Rajchl, "Stratified decision forests for accurate anatomical landmark localization in cardiac images," *IEEE Transactions on Medical Imaging*, vol. 36, no. 1, pp. 332–342, 2017.
- [13] A. V. Nikolaev, L. D. Jong, G. Weijers, and V. Groenhuis, "Quantitative evaluation of an automated cone-based breast ultrasound scanner for MRI–3D US image fusion," *IEEE Transactions on Medical Imaging*, vol. 40, no. 4, pp. 1229–1239, 2021.
- [14] H. Bogunović, F. Venhuizen, and S. Klimescha, "RETOUCH: the retinal OCT fluid detection and segmentation benchmark and challenge," *IEEE Transactions on Medical Imaging*, vol. 38, no. 8, pp. 1858–1874, 2019.
- [15] O. Oktay, E. Ferrante, K. Kamnitsas, and M. Heinrich, "Anatomically constrained neural networks (ACNNs): application to cardiac image enhancement and segmentation," *IEEE Transactions on Medical Imaging*, vol. 37, no. 2, pp. 384–395, 2018.
- [16] W. Xianghong, Y. Shi-e, and X. Xincheng, "An effective method to colour medical image enhancement," in *Proceedings of the IEEE/ICME International Conference on Complex Medical Engineering*, pp. 874–877, Beijing, China, May, 2007.
- [17] N. Weng, Y. Yang, and R. Pierson, "Three-dimensional surface reconstruction using optical flow for medical imaging," *IEEE Transactions on Medical Imaging*, vol. 16, no. 5, pp. 630–641, 1997.
- [18] M. J. J. P. van Grinsven, B. van Ginneken, C. B. Hoyng, T. Theelen, and C. I. Sánchez, "Fast convolutional neural network training using selective data sampling: application to hemorrhage detection in color fundus images," *IEEE Transactions on Medical Imaging*, vol. 35, no. 5, pp. 1273–1284, 2016.
- [19] G. V. Pendse, R. Baumgartner, A. J. Schwarz, A. Coimbra, D. Borsook, and L. Becerra, "A statistical framework for optimal design matrix generation with application to fMRI," *IEEE Transactions on Medical Imaging*, vol. 29, no. 9, pp. 1573–1611, 2010.
- [20] S. Kostopoulos, D. Cavouras, A. Daskalakis, and P. Bougioukos, "Colour-Texture based image analysis method for assessing the Hormone Receptors status in Breast tissue sections," in *Proceedings of the 29th Annual International Conference of the IEEE Engineering in Medicine and Biology Society*, pp. 4985–4988, Lyon, France, August 2007.
- [21] C. H. Li and P. C. Yuen, "Regularized color clustering in medical image database," *IEEE Transactions on Medical Imaging*, vol. 19, no. 11, pp. 1150–1155, Nov, 2000.
- [22] A. S. Panayides, A. Amini, N. D. Filipovic, and A. Sharma, "AI in medical imaging informatics: current challenges and future directions," *IEEE Journal of Biomedical and Health Informatics*, vol. 24, no. 7, pp. 1837–1857, 2020.
- [23] M. Geng, X. Meng, J. Yu, L. Zhu, and L. Jin, "Content-noise complementary learning for medical image denoising," *IEEE Transactions on Medical Imaging*.
- [24] S. M. Pizer, "The medical image display and analysis group at the university of North Carolina: reminiscences and philosophy," *IEEE Transactions on Medical Imaging*, vol. 22, no. 1, pp. 2–10, 2003.
- [25] C. Vertan and G. Voicea, "A comparison of decolorization methods performance for medical color images," in *Proceedings of the E-Health and Bioengineering Conference (EHB)*, pp. 1–4, November, 2015.
- [26] J. Kim, W. Cai, D. Feng, and H. Wu, "A new way for multidimensional medical data management: volume of interest (VOI)-Based retrieval of medical images with visual and functional features," *IEEE Transactions on Information Technology in Biomedicine*, vol. 10, no. 3, pp. 598–607, 2006.
- [27] H. Xu, C. Li, M. M. Rahaman, Y. Yao, and Z. Li, "An enhanced framework of generative adversarial networks (EF-GANs) for environmental microorganism image augmentation with limited rotation-invariant training data," *IEEE Access*, vol. 8, Article ID 187455, 2020.
- [28] W. Yang and J.-R. Liu, "Research and development of medical image fusion," in *Proceedings of the IEEE International Conference on Medical Imaging Physics and Engineering*, pp. 307–309, Shenyang, China, October 2013.
- [29] Y. Chen, Z. Li, L. Wang, N. Wang, and B. Hong, "High-capacity reversible watermarking algorithm based on the region of interest of medical images," in *Proceedings of the 14th IEEE International Conference on Signal Processing (ICSP)*, pp. 1158–1162, Beijing, China, August 2018.
- [30] K. Gong, K. Kim, D. Wu, M. K. Kalra, and Q. Li, "Low-dose dual energy CT image reconstruction using non-local deep image prior," in *Proceedings of the IEEE Nuclear Science Symposium and Medical Imaging Conference (NSS/MIC)*, pp. 1–2, Manchester, UK, October 2019.